Cancer Letters 601 (2024) 217177

Contents lists available at ScienceDirect

Cancer Letters

journal homepage: www.elsevier.com/locate/canlet

Original Articles

6-Phosphogluconate dehydrogenase promotes glycolysis and fatty acid synthesis by inhibiting the AMPK pathway in lung adenocarcinoma cells

Jun Wu [a,c,g,1], Yong Chen [d,1], Hui Zou [b,c,1], Kaiyue Xu [e,1], Jiaqi Hou [f], Mengmeng Wang [f], Shuyu Tian [f], Mingjun Gao [f], Qinglin Ren [f], Chao Sun [c], Shichun Lu [c], Qiang Wang [h], Yusheng Shu [b,c,g,***], Shouyu Wang [h,**], Xiaolin Wang [a,c,g,*]

[a] Medical College, Yangzhou University, Yangzhou, China
[b] The Yangzhou School of Clinical Medicine of Nanjing Medical University, Yangzhou, China
[c] Department of Thoracic Surgery, Northern Jiangsu People's Hospital, Yangzhou, China
[d] Department of Thoracic Surgery, Sichuan Cancer Hospital & Institute, Sichuan Cancer Center, School of Medicine, University of Electronic Science and Technology of China, Chengdu, China
[e] Department of Radiation Oncology, Suzhou Municipal Hospital, Suzhou, China
[f] First College of Clinical Medicine, Dalian Medical University, Dalian, China
[g] Yangzhou Key Laboratory of Thoracic and Cardiac Surgery, Yangzhou, China
[h] Department of Hepatobiliary Surgery, The First Affiliated Hospital of Anhui Medical University, Anhui Provincial Innovation Institute for Pharmaceutical Basic Research, Innovative Institute of Tumor Immunity and Medicine (ITIM), Anhui Province Key Laboratory of Tumor Immune Microenvironment and Immunotherapy, Hefei, China

ARTICLE INFO

Keywords:
Lung adenocarcinoma
Single-cell sequencing
Pentose phosphate pathway
6-Phosphogluconate dehydrogenase
AMPK pathway

ABSTRACT

Abnormal metabolism has emerged as a prominent hallmark of cancer and plays a pivotal role in carcinogenesis and progression of lung adenocarcinoma (LUAD). In this study, single-cell sequencing revealed that the metabolic enzyme 6-phosphogluconate dehydrogenase (PGD), which is a critical regulator of the pentose phosphate pathway (PPP), is significantly upregulated in the malignant epithelial cell subpopulation during malignant progression. However, the precise functional significance of PGD in LUAD and its underlying mechanisms remain elusive. Through the integration of TCGA database analysis and LUAD tissue microarray data, it was found that PGD expression was significantly upregulated in LUAD and closely correlated with a poor prognosis in LUAD patients. Moreover, in vitro and in vivo analyses demonstrated that PGD knockout and inhibition of its activity mitigated the proliferation, migration, and invasion of LUAD cells. Mechanistically, immunoprecipitation-mass spectrometry (IP-MS) revealed for the first time that IQGAP1 is a robust novel interacting protein of PGD. PGD decreased p-AMPK levels by competitively interacting with the IQ domain of the known AMPKα binding partner IQGAP1, which promoted glycolysis and fatty acid synthesis in LUAD cells. Furthermore, we demonstrated that the combination of Physcion (a PGD-specific inhibitor) and metformin (an AMPK agonist) could

Abbreviations: LUAD, lung adenocarcinoma; LUSC, lung squamous cell carcinoma; NSCLC, non-small cell lung cancer; OS, overall survival; PGD, 6-phosphogluconate dehydrogenase; PPP, pentose phosphate pathway; PVDF, polyvinylidene fluoride; qRT–PCR, quantitative real-time polymerase chain reaction; ROS, reactive oxygen species; RT, reverse transcription; Ru5P, ribulose-5-phosphate; SD, standard deviation; SDS–PAGE, sodium dodecyl sulfate–polyacrylamide gel electrophoresis; TCGA, The Cancer Genome Atlas; TMA, tissue microarray; TME, tumor microenvironment; UMAP, uniform manifold approximation and projection; 2-DG, 2-deoxy-glucose; CCK-8, Cell Counting Kit-8; DAB, 3, 3′-diaminobenzidine; DAPI, 4′,6-diamidino-2-phenylindole; AMPK, AMP-activated protein kinase; DCFH-DA, 2′,7′-dichlorofluorescein diacetate; DTT, dithiothreitol; ECAR, extracellular acidification rate; ECL, enhanced chemiluminescence; FBS, fetal bovine serum; FACS, fluorescence-assisted cell sorting; GSEA, gene set enrichment analysis; GSVA, gene set variation analysis; HRP, horseradish peroxidase; IAA, 2-iodoacetamide; IF, immunofluorescence; IHC, immunohistochemistry; IP, immunoprecipitation; IRS, immunoreactivity score; KEGG, Kyoto Encyclopedia of Genes and Genomes; LC-MS/MS, liquid chromatography-tandem mass spectrometry.

* Corresponding author. Medical College, Yangzhou University, Yangzhou, China.
** Corresponding author. Department of Hepatobiliary Surgery, The First Affiliated Hospital of Anhui Medical University, Anhui Provincial Innovation Institute for Pharmaceutical Basic Research, Innovative Institute of Tumor Immunity and Medicine (ITIM), Anhui Province Key Laboratory of Tumor Immune Microenvironment and Immunotherapy, Hefei, China.
*** Corresponding author. The Yangzhou School of Clinical Medicine of Nanjing Medical University, Yangzhou, China.
E-mail addresses: 18051061999@yzu.edu.cn (Y. Shu), shouyuwang@ahmu.edu.cn (S. Wang), 18051063909@yzu.edu.cn (X. Wang).
[1] These authors contributed equally to this article.

https://doi.org/10.1016/j.canlet.2024.217177
Received 25 April 2024; Received in revised form 27 July 2024; Accepted 5 August 2024
Available online 22 August 2024
0304-3835/© 2024 The Authors. Published by Elsevier B.V. This is an open access article under the CC BY-NC-ND license (http://creativecommons.org/licenses/by-nc-nd/4.0/).

inhibit tumor growth more effectively both in vivo and in vitro. Collectively, these findings suggest that PGD is a potential prognostic biomarker and therapeutic target for LUAD.

1. Introduction

Non-small cell lung cancer (NSCLC) is the most common cause of cancer-related mortality, causing millions of deaths every year worldwide. Among the various pathological types of NSCLC, lung adenocarcinoma (LUAD) has emerged as the predominant type [1,2]. Despite the continual advancements in LUAD treatment [3], efficacy remains disconcertingly marginal. Thus, it is crucial to identify a definitive biological marker for LUAD diagnosis and prognosis evaluation. Metabolic perturbations are emerging as key events in tumorigenesis and cancer growth [4,5]. The pentose phosphate pathway (PPP) plays a pivotal role in helping cancer cells meet anabolic demands and combat oxidative stress [6]. The aberrant activation of the PPP in tumor cells results in pentose phosphate production, promoting nucleic acid synthesis and increasing the levels of NADPH, which is essential for fatty acid synthesis and cell viability under stressful conditions [7,8]. Thus, targeting the PPP remains an attractive therapeutic intervention in cancer. 6-Phosphogluconate dehydrogenase (PGD), the third enzyme in the PPP, generates the second NADPH molecule and ribulose-5-phosphate (Ru5P). PGD plays an instrumental role in the malignant progression of tumors. Abolishing the phosphorylation of PGD significantly reduces EGF-induced glioma cell proliferation, tumor growth, and resistance to ionizing radiation [9]. Furthermore, ATP13A2 activates the PPP to promote colorectal cancer growth through the TFEB-PGD axis [10]. A reciprocal interaction between the androgen receptor and PGD also promotes the proliferation of prostate cancer cells [11]. However, its functional role in LUAD progression remains unknown.

IQGAP1 is a scaffold that regulates several biological processes and metabolic pathways by interacting with its binding partners [12]. The interaction between ARF1 and IQGAP1, which reactivates ERK signaling, plays a crucial role in vemurafenib resistance and colorectal cancer metastasis [13]. Moreover, direct interactions between IQGAP1 and both AMPK and CaMKK2 suppress AMPK activation in various cell types [14]. Nevertheless, very few previous studies have reported the impact of alterations in IQGAP1-associated interactions in LUAD.

In the present study, we identified the high expression of PGD and its biological role in LUAD. Mechanistically, it was found that PGD competitively interacts with the IQ domain of IQGAP1, which activates the AMPK pathway and promotes glycolysis and fatty acid synthesis in LUAD cells. Our findings demonstrate that PGD may be a promising predictive biomarker for patients with LUAD in the clinic.

2. Materials and methods

2.1. Patients and specimens

Lung cancer specimens and matched adjacent tissues were obtained from patients at the Northern Jiangsu People's Hospital and used to construct a tissue microarray. The microarray cohort (n = 62) comprised patients with adenocarcinomas (n = 21) and squamous cell carcinomas (n = 41). Patients treated with radical gastrectomy, adjuvant radiotherapy, or chemotherapy during the observation period were excluded. Ethical approval was obtained from the Ethics Committee of Northern Jiangsu People's Hospital.

2.2. Single-cell sequencing

Specimens were collected from six patients with primary LUAD who were first examined and underwent surgery at the Department of Thoracic Surgery, Northern Jiangsu People's Hospital. Thirteen samples were collected, consisting of one normal tissue sample and 12 tumor tissue samples. Tissues were digested into single cells and loaded onto the 10x Genomics Chromium™ platform. Single-cell RNA-Seq libraries were prepared using the 10x Genomics Chromium Next GEM Single Cell 3' Kit v3.1 according to the manufacturer's protocol. Indexed libraries were pooled according to the number of cells and sequenced on a NovaSeq 6000 (Illumina) using 150-bp paired ends. The output-filtered gene expression matrices were analyzed using the Seurat software package (v.4.3.0) in R software (v.4.3.0).

2.3. Cell lines and drugs

Four human lung cancer cell lines (A549, PC9, SPCA1 and H1975) and one normal human lung cell line (B2B) were obtained from the American Type Culture Collection (ATCC, MD, VA, US) and cultured according to the ATCC instructions. Physcion, metformin, and dorsomorphin dihydrochloride were purchased from MedChemExpress (Shanghai, China).

2.4. Cell transduction

SgRNAs targeting PGD and PGD Flag-tagged lentiviruses were designed and synthesized by Corues Biotechnology (Nanjing, China). For transduction, the cells were plated at approximately 30–40 % confluence in 6-well plates. After 72 h of transduction, the cells were harvested and used for further experiments. The sequences of the sgRNAs used were as follows: sg-PGD_001, 5′-GGCCAAGAAATCATCAACTT-3′; sg-PGD_002, 5′-GGCCAAGAAATCATCAACTT-3′; and sg-PGD_003, 5′-ACCAGGAGGATGATCCGCCG-3′.

2.5. Animal model

B6-Kras$^{LSL\text{-}G12D/+}$ mice were obtained from Jiangsu GemPharmatech (Nanjing, China) and bred under specific-pathogen-free (SPF) conditions. After being anesthetized with 4 % chloral hydrate, the mice were intratracheally injected with 5×10^7 PFU of adenovirus (Ad-Cre, OBIO) at 4–6 weeks of age and sacrificed 24 weeks after infection.

BALB/cJGpt mice (4–5 weeks old) were purchased from GemPharmatech (Nanjing, China) and divided into four groups. After subcutaneous implantation of A549 cells, the mice were intragastrically administered PBS, Physcion (20 mg/kg), metformin (10 mg/kg), or a combination of the two drugs once every 2 days, at the tumor volume of 20 mm^3. Tumor weight and tumor size were recorded every four days, and the tumor volume was calculated as $\pi/6 \times L \times W^2$ (W, width at the widest point; L, perpendicular width). Xenograft tumors were harvested after 6 weeks.

All animal experiments were approved by the Ethics Committee of North Jiangsu People's Hospital (Yangzhou, China).

2.6. Cell viability assay

Cells were seeded at a density of 2×10^3 cells/well in 96-well plates. Viability was assessed after culture for 0, 24, and 48 h using a CCK-8 assay (Dojindo Laboratories, Japan); the cells were incubated with the CCK-8 reagent for 1 h at 37 °C. The absorbance of the cells was measured at 450 nm using a microplate reader. Different concentrations of Physcion were added to the wells, followed by incubation for 48 h. Cell proliferation was detected in the same way as described above.

2.7. Colony formation assay

Five hundred LC cells were seeded in 6-well plates and transfected or

cultured with Physcion at different concentrations. After 14 days, the cells were fixed with 4 % formaldehyde for 10 min and stained with crystal violet at room temperature for 30 min. Then, the cells were washed twice with PBS and observed under a microscope.

2.8. Cell migration and invasion assay

Transwell chambers (Corning, NY, USA) with or without Matrigel (Mogengel Bio #082704, Xiamen, China) were used to detect cell migration and invasion. Briefly, 1×10^4 cells were seeded in the upper Transwell chamber in serum-free medium. The lower chamber was incubated with complete medium supplemented with 20 % fetal bovine serum (FBS) at 37 °C. After 24 h, nonmigratory or noninvasive cells were removed, and the cells that migrated through the membrane were counted under a microscope (Olympus, Tokyo, Japan) after fixation and staining with crystal violet.

2.9. Spheroid formation and invasion assay

Five thousand cells were seeded in a 96-well ultralow attachment plate (Corning #3474, NY, USA) containing RPMI 1640 medium supplemented with 10 % FBS for three-dimensional (3D) culture. After 48 h, spheroids were established in 96-well plates, and half of the medium was replaced with Matrigel (Mogengel Bio #082704, Xiamen, China) for the invasion assay. After a 96-h incubation period, the formed spheroids were imaged using a microscope (Olympus, Tokyo, Japan).

2.10. Bioinformatics and statistical analysis

The RNA expression data of 585 LUAD patients and 550 LUSC

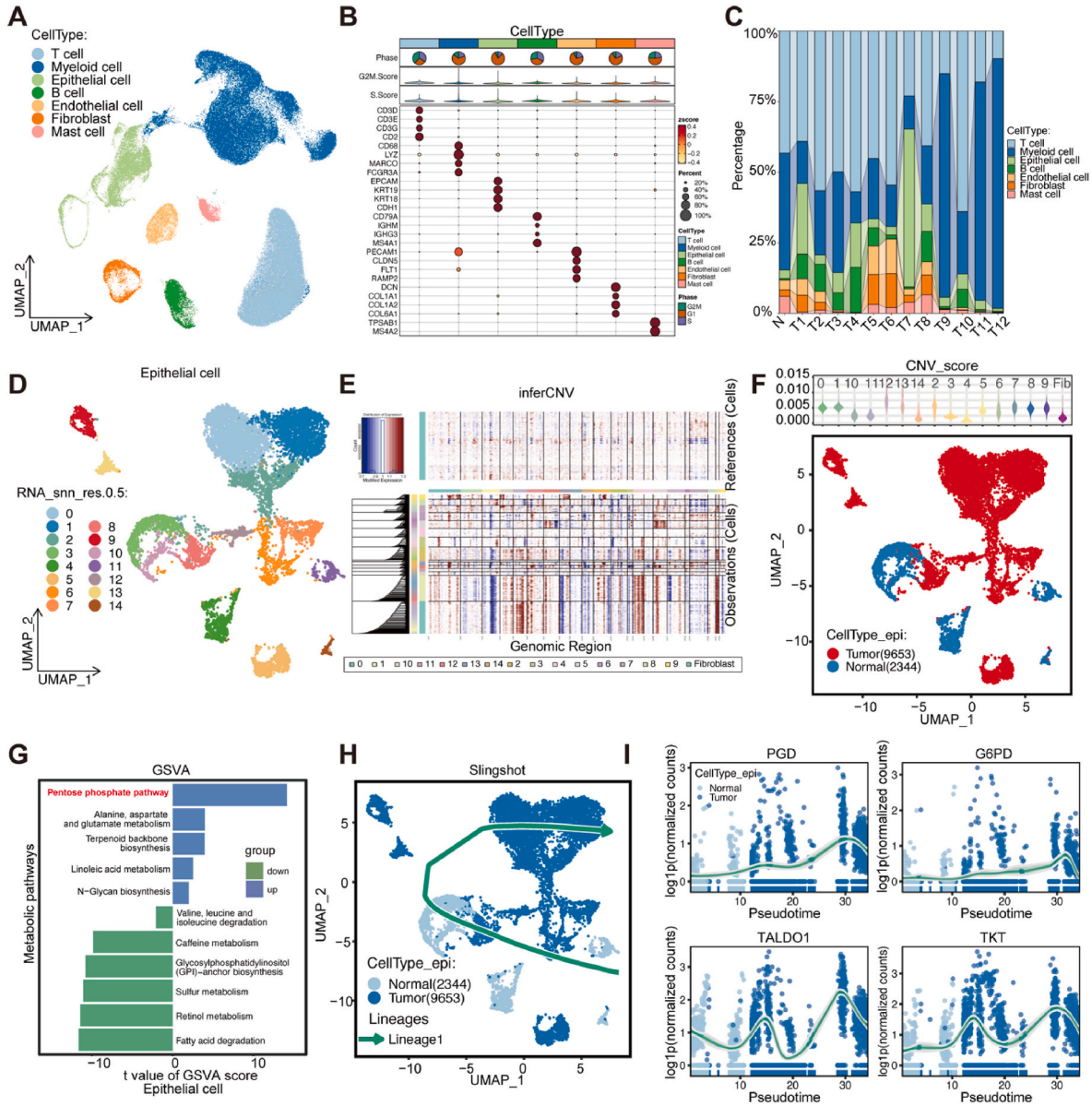

Fig. 1. Single-cell sequencing revealed significant activation of the PPP in malignant epithelial cells in LUAD. (A) Global uniform manifold approximation and projection (UMAP) plot of 7 cell types comprising 143,382 cells obtained via scRNA-seq. (B) Heatmap depicting marker genes of each cell type. (C) Cell proportion diagram of each sample. (D) Global UMAP plot of 15 clusters of epithelial cells. (E) CNVs in epithelial cells compared with those in fibroblasts. The red color represents amplification, and the blue color represents deletion. (F) Global UMAP plot of epithelial cells defined as either normal or tumor cells based on the CNVscore. (G) T values calculated via GSVA and the limma package based on metabolic pathway-related gene sets. (H) Pseudotime analysis of all epithelial cells via Slingshot. (I) Pseudotime analysis of four rate-limiting enzymes in the PPP pathway via Slingshot.

patients were downloaded from The Cancer Genome Atlas (TCGA) database (https://portal.gdc.cancer.gov/) and analyzed using DESeq2. Metabolism-related gene sets were selected from the Gene Set Enrichment Analysis (GSEA) database, and gene set variation analysis (GSVA) was performed to evaluate metabolic pathway activity. Statistical analyses were conducted using a two-tailed unpaired Student's *t*-test unless otherwise indicated. All the data are presented as the means ± standard deviations (SDs) of three independent experiments. The significance level is indicated as follows: *P < 0.05, **P < 0.01, ***P < 0.001, and ****P < 0.0001. Overall survival (OS) (from the date of surgery to the date of death) was analyzed using Kaplan–Meier curves. SPSS software (version 19.00) was used for the statistical analysis.

3. Results

3.1. The PPP is significantly activated in LUAD

The tumor microenvironment (TME) is an indispensable factor in tumorigenesis and development[15–18]. To explore the cellular and molecular heterogeneity in LUAD, we collected one normal tissue sample and twelve tumor tissue samples from six LUAD patients for single-cell RNA sequencing. After processing and quality control of the raw data, 143382 cells were retained for subsequent analysis. We employed the Harmony algorithm to harmonize the data and ensure robust downstream analyses to mitigate the confounding effects of batch variations. Based on the expression of canonical marker genes, we accurately annotated each cell as a T cell (*CD3D, CD3E, CD3G,* and *CD2*), a myeloid cell (*CD68*, *LYZ*, *MARCO*, and *FCGR3A*), an epithelial cell (*EPCAM*, *KRT19*, *KRT18*, and *CDH1*), a B cell (*CD79A*, *IGHM*, *IGHG3*, and *MS4A1*), an endothelial cell (*PECAM1*, *CLDN5*, *FLT1*, and *RAMP2)*, a fibroblast (*DCN*, *COL1A1*, *COL1A2*, and *COL6A1*), or a mast cell (*TPSAB1* and *MS4A2)* and subsequently visualized the cellular landscape using a UMAP plot (Fig. 1A–C). Specifically focusing on the epithelial cell population, we classified them into 15 clusters and employed the inferCNV algorithm to investigate chromosomal copy number variations (CNVs) at the single-cell level. Fibroblasts were used as reference cells since they have low CNVs in LUAD. We stratified the epithelial cells into normal and tumor categories by calculating the CNV score for each cluster (Fig. 1D–F). Dysregulation of tumor metabolism plays a crucial role in the malignant transformation of tumors [19]; thus, we conducted a gene set variation analysis (GSVA) based on metabolic pathway-related gene sets downloaded from the Molecular Signatures Database (MSigDB) [20], which revealed significant upregulation of genes in the PPP, specifically within the malignant epithelial cell subset

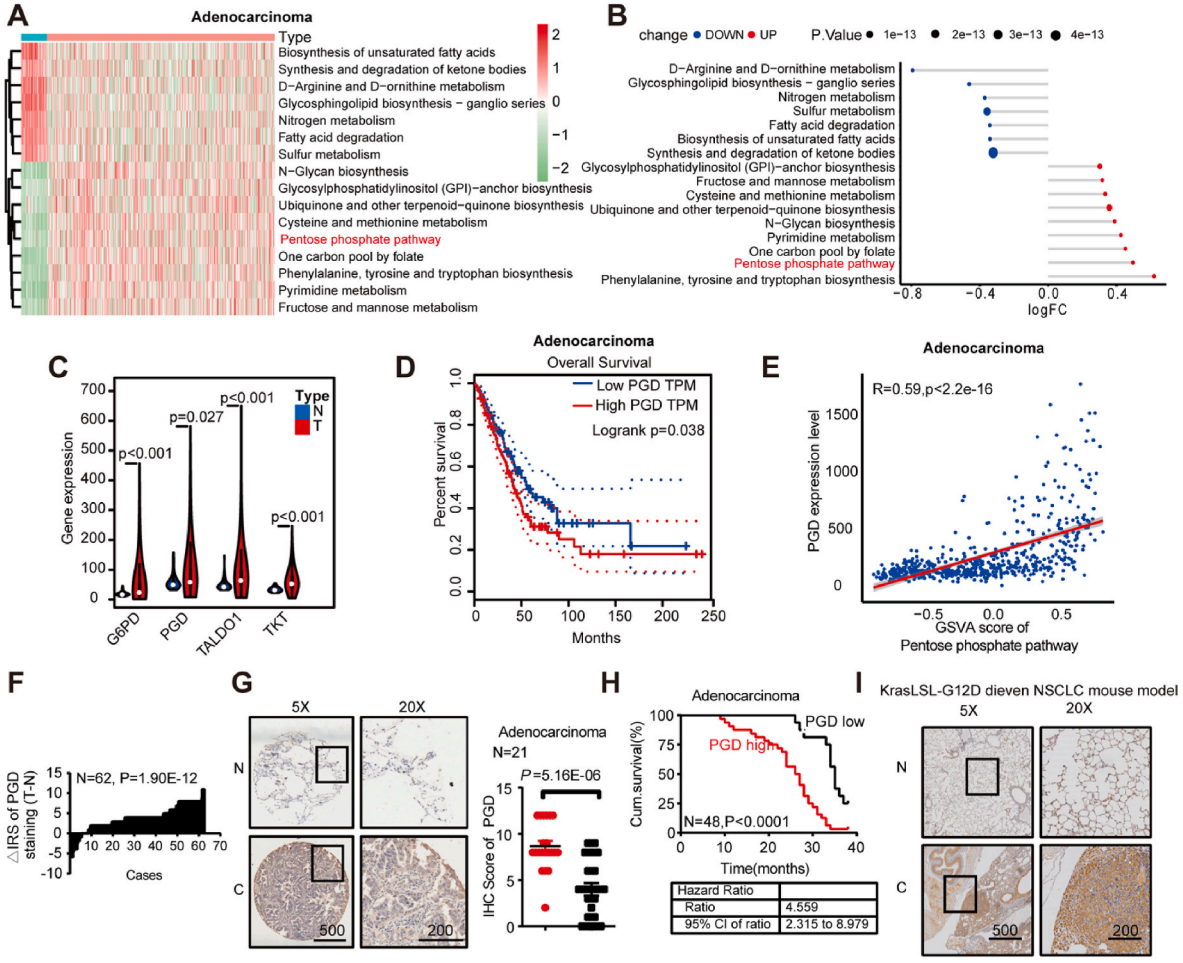

Fig. 2. The expression of PGD was significantly upregulated in LUAD and was associated with a poor prognosis. (A) GSVA was used to score the differentially expressed metabolic pathway-related gene sets for each sample, and the values were compared between the normal and tumor tissues from the TCGA. (B) Lollipop plot depicting the GSVA score of metabolism-associated genes in each sample between the normal and tumor tissues. (C) Violin plot of four rate-limiting enzymes in the PPP pathway. (D) Kaplan–Meier analysis of the overall survival (OS) profiles of the TCGA LUAD cohort. (E) Spearman's correlation analysis of the correlation between the expression of PGD and GSVA scores of PPP pathway-associated genes. (F) The distribution of the difference in the PGD immunoreactivity score (IRS) (△IRS=IRST−IRSN). The IRS of PGD staining was available for 62 pairs of tissues. (G) Representative IHC images of 21 pairs of LUAD tissues in the tissue microarray (TMA) probed with anti-PGD antibodies (scale bars = 500 μm or 50 μm). (H) Kaplan–Meier analysis of OS based on PGD expression in patients with LUAD. (I) Representative IHC images of tissues from LUAD orthotopic models probed with anti-PGD antibodies (scale bars = 500 μm or 50 μm).

(Fig. 1G). Furthermore, we employed the slingshot algorithm to calculate the trajectory of epithelial cells and assessed the core molecules involved in PPP-driven tumorigenesis [21]. The expression levels of rate-limiting enzymes (PGD, G6PD, TALDO1, and TKT) in the PPP progressively increased during the transition of epithelial cells from a benign state to a malignant state (Fig. 1H and I). These findings suggest that the PPP plays a critical role in the tumorigenesis and development of LUAD.

3.2. PGD is highly expressed in LUAD and associated with poor prognosis

To further validate these findings, we downloaded TCGA data for 568 LUAD patients and 545 LUSC patients. Then, GSVA based on metabolic pathway-related gene sets was conducted, and the results showed that the PPP was also significantly enriched in both LUSC and LUAD samples compared to the controls (Fig. 2A and B; Figs. S1B and C). Moreover, the expression of all four rate-limiting enzymes (PGD, G6PD, TALDO1, and TKT) was significantly elevated (Fig. 2C; Figs. S1D and E). However, only high expression of PGD was associated with a poor prognosis in LUAD patients but not in LUSC patients. These findings highlight the potential role of PGD in the pathogenesis of LUAD and underscore its relevance as a prognostic marker for LUAD patients (Fig. 2D; Figs. S1A and G). The robust correlation between PPP activity and high PGD expression further validated this observation (Fig. 2E; Fig. S1F).

Next, a tissue microarray (TMA) was constructed, and PGD staining was performed via immunohistochemistry to further elucidate the expression pattern of PGD in LUAD. PGD expression was greater in cancerous tissues than in paired normal tissues from LUAD and LUSC patients. Consistently, high PGD levels were positively associated with worse prognosis in LUAD patients but not in LUSC patients (Fig. 2F–H; Figs. S1H–J). To further confirm this finding, a murine orthotopic LUAD model was established using B6-Kras$^{LSL\text{-}G12D}$ mice, and cancer and adjacent normal tissues were collected (Fig. 2I). The IHC results showed that PGD was significantly upregulated in tumor tissues compared to normal tissues, indicating that PGD may act as an oncogene in LUAD and accelerate the progression of LUAD.

3.3. PGD promotes the proliferation, migration, and invasion of LUAD cells

We first assessed PGD expression in a human normal lung bronchial epithelial cell line (BEAS-2B) and four LUAD cell lines (A549, SPCA1, H1975 and PC9). The results revealed that the protein level of PGD was significantly greater in LUAD cells than in BEAS-2B cells. Furthermore, to assess the function of PGD in LUAD, we established A549 cells with stable PGD knockout and H1975 cells with stable PGD overexpression (Fig. 3A; Fig. S2A). The upregulation of PGD significantly promoted H1975 cell viability, while the knockout of PGD decreased A549 cell viability according to the CCK-8 assay (Fig. 3B and C; Figs. S2B and C). Consistently, colony formation assays showed that PGD overexpression markedly promoted LUAD cell colony formation, while PGD deficiency inhibited colony formation (Fig. 3D and E; Fig. S2D). These data suggest that PGD may act as an oncogene that promotes LUAD cell proliferation.

Next, to determine the role of PGD in LUAD cell metastasis, we first performed migration and invasion assays in vitro. The data showed that ectopic expression of PGD promoted the migration and invasion of H1975 cells. Conversely, PGD knockout in A549 cells had the opposite effect (Figs. S2E–G). To further evaluate the role of PGD expression in invasion, cells were seeded in ultralow attachment plates, and tumor cell spheroids were formed after 48 h. Then, we embedded tumor cell spheroids in Matrigel and evaluated their invasive potential. A549 cells with PGD knockout were not able to invade Matrigel. Similarly, compared with control H1975 cells, PGD-overexpressing H1975 cells had increased Matrigel invasion capacity (Fig. 3F and G). Therefore, these data indicate the critical role of PGD in promoting LUAD cell metastasis.

In addition, Physcion, an anthraquinone isolated from the traditional Chinese medicine Radix et Rhizoma Rhei, is an inhibitor of PGD [8]. Thus, we treated LUAD cell lines with different doses of Physcion for 48 h and found that cell viability decreased in a dose-dependent manner ($p < 0.05$) (Fig. 3H; Fig. S3A). Next, a colony formation assay was performed, and the results showed that Physcion significantly suppressed the colony formation of LUAD cells (Fig. 3I; Fig. S3C). Furthermore, Transwell assays revealed that 50 μM Physcion treatment markedly reduced the migratory and invasive abilities of LUAD cells (Fig. 3K and L; Fig. S3D). However, 50 μM Physcion did not affect the proliferation of LUAD cells after 12 h (Fig. 3J). We also performed tumor xenograft studies to verify the roles of PGD in vivo, and the results showed that knockout of PGD significantly inhibited tumor growth, as reflected by the tumor size and weight compared with those of tumors derived from the WT cells (Fig. 3M–O). In addition, IHC results showed decreased expression of Ki-67, a biomarker of proliferation, in the tumor tissues of the PGD knockout group compared with that in the WT group (Fig. 3P). Collectively, these results demonstrated that PGD is essential for the proliferation, migration, and invasion of LUAD cells in vitro and in vivo.

3.4. Inhibition of PGD decreases enzyme activity and inhibits glycolysis and fatty acid synthesis

PGD catalyzes the decarboxylation of 6-phosphogluconate, yielding Ru-5-P and NADPH to fulfill the unique bioenergetic and biosynthetic demands of cancer cells [22]. In our study, we found that PGD knockout or Physcion treatment decreased the NADPH/NADP$^+$ ratio (Fig. 4D; Fig. S3B). Reactive oxygen species (ROS) produced by various biochemical and physiological oxidative processes in the body are associated with numerous physiological and pathophysiological processes and play a major role in the pathogenesis of cancer [23–25]. In particular, the NAPDH oxidase family is considered an important regulator of ROS generation [26]. Knockout of PGD or treatment with Physcion significantly increased the ROS levels in A549 and SPCA cells. Notably, Physcion significantly increased ROS levels in a dose-dependent manner (Fig. 4A–C; Figs. S4A and B).

Next, to identify the molecular mechanism by which PGD promotes LUAD progression, we divided tumor epithelial cells into two groups based on PGD expression levels and performed gene set enrichment analysis (GSEA) based on the Kyoto Encyclopedia of Genes and Genomes (KEGG) dataset. The results indicated that the adipocytokine signaling pathway and glycolysis pathway were significantly enriched in PGD-high cells (Fig. 4E). We further substantiated this finding through experimental verification. Knockout of PGD in A549 cells markedly suppressed lactate production and decreased glycolytic capacity (Fig. 4F and G). In contrast, PGD upregulation significantly promoted lactate production and increased glycolytic capacity in H1975 cells. Oil Red O staining also revealed that PGD expression significantly promoted lipid accumulation in H1975 cells (Fig. 4H). Knockout of PGD in A549 cells induced the opposite effects. Collectively, these findings suggest that PGD may promote glycolysis and lipid metabolism to drive LUAD progression.

3.5. PGD inhibits the activation of the AMPK pathway by competitively interacting with IQGAP1

AMP-activated protein kinase (AMPK) is an AMP-sensitive protein kinase that functions as an energy stress sensor in cells and plays a key role in the regulation of energy homeostasis, including glycolysis and fatty acid synthesis [27–29]. Previous studies have also shown that LKB1-AMPK activation is mediated by the Ru-5-P level, which depends on PGD activity in tumors [8,30,31]. We speculated that PGD may also regulate the AMPK pathway in LUAD. The Western blotting results showed that the p-AMPK level was markedly increased in LUAD cells after the inhibition of PGD activity (Fig. 5A).

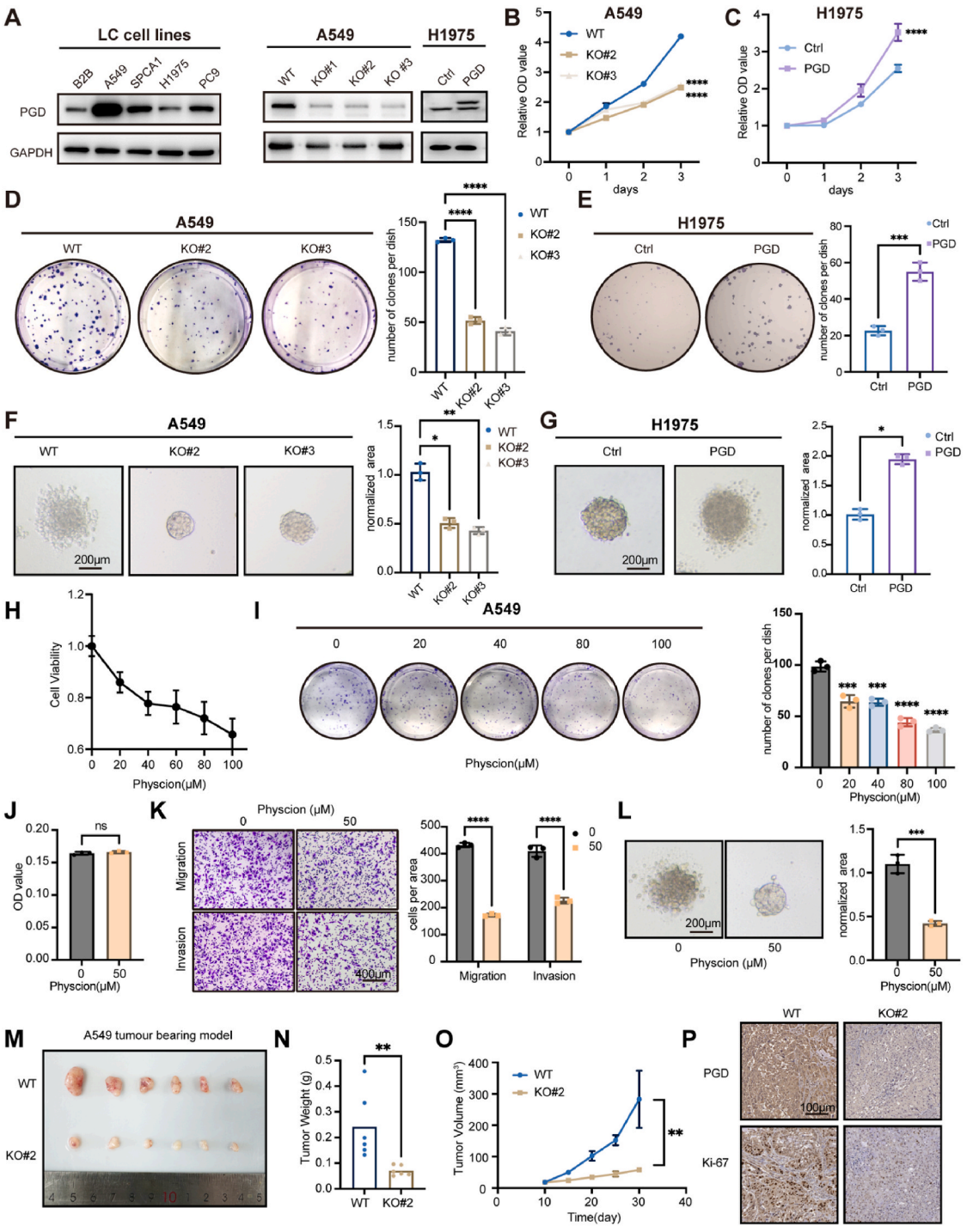

Fig. 3. PGD promotes the proliferation, migration, and invasion of LUAD cells in vitro and in vivo. (A) The protein levels of PGD in a human normal lung bronchial epithelial cell line (BEAS-2B) and four LUAD cell lines were measured by WB. The efficiency of PGD knockout and overexpression was verified at the protein level by WB in A549 and H1975 cells. (B, C) The knockout of PGD significantly decreased A549 cell viability, while the upregulation of PGD increased H1975 cell viability according to the CCK-8 assay. (D) The knockout of PGD impaired the colony formation ability of A549 cells (left panel). Quantification of the colony formation assay results (right panel). (E) Overexpression of PGD increased the colony-forming ability of H1975 cells (left panel). Quantification of the colony formation assay results (right panel). (F, G) Invasion of A549 cells (F) and H1975 cells (G) after knockout or overexpression of PGD 48 h after embedding the spheroids in Matrigel. The area occupied by spheroids embedded in Matrigel was quantified as a readout of invasion, and representative images are shown. Scale bar = 200 μm. (H, I) Physcion dose-dependently decreased the viability (H) and the colony formation ability (I) of A549 cells. (J–K) Physcion did not affect the viability of A549 cells at a concentration of 50 μM (J) but significantly inhibited the migration and invasion abilities of A549 cells in transwell chambers (L). Representative images (scale bars = 400 μm, left panel) and quantification (right panel) of the cell migration and invasion assay results are shown. (L) Invasion of A549 cells into Matrigel using Physcion (50 μM). The area occupied by spheroids embedded in Matrigel was quantified as a readout of invasion, and representative images are shown. Scale bar = 200 μm. (M) Knockout of PGD inhibited A549 LUAD cells subcutaneous tumor growth in nude mice (n = 6). (N) The tumors were extracted and weighed after 30 days. (O) The tumor volume was monitored every five days, and tumor growth curves were generated. (P) Sections of tumors were stained with anti-Ki-67 and anti-PGD antibodies by IHC (scale bars = 100 μm).

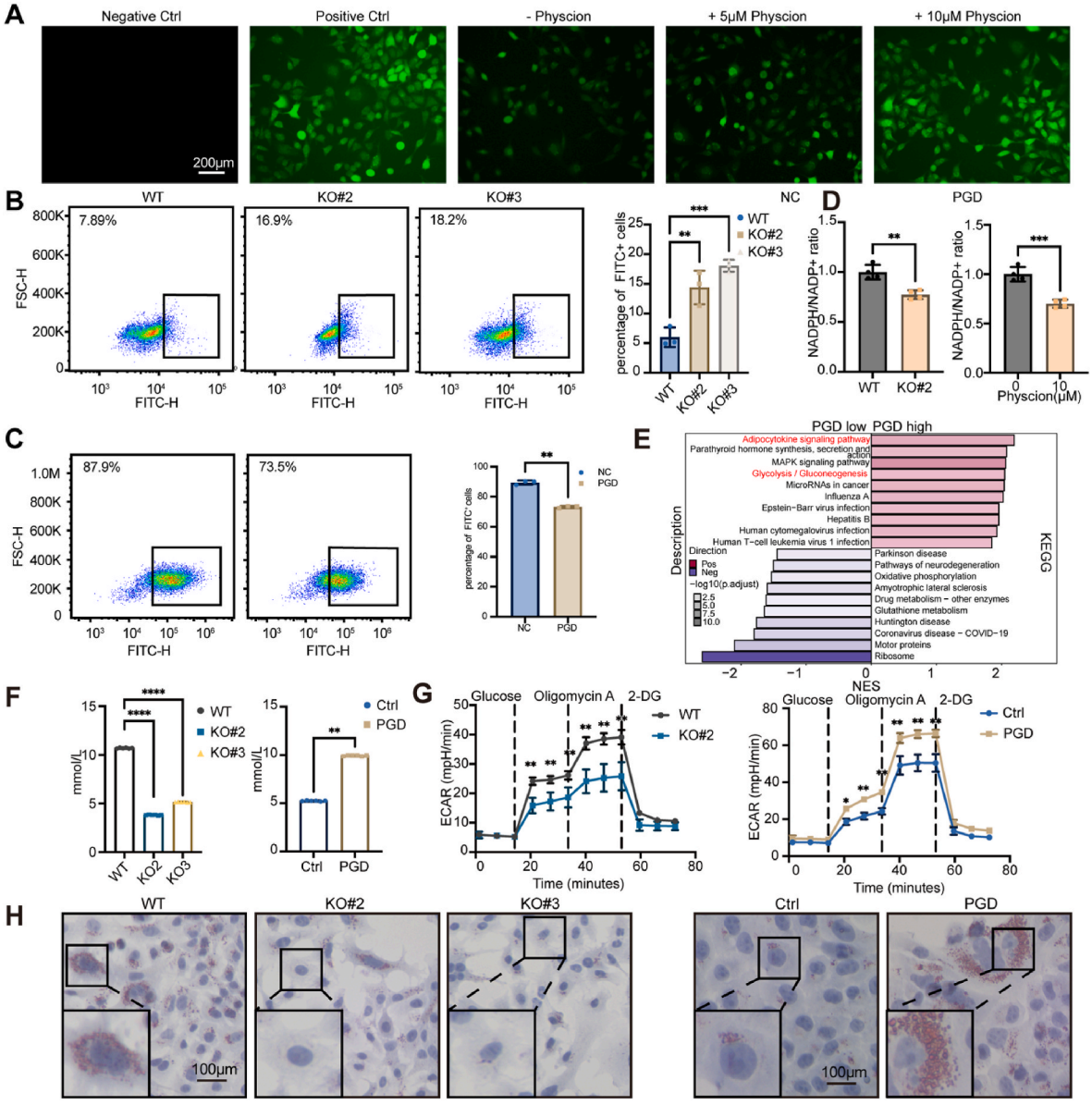

Fig. 4. PGD accelerates LUAD malignant progression by inhibiting glycolysis and fatty acid synthesis. (A) After adding different concentrations of Physcion to A549 cells, the cells were incubated with DCFH-DA, and the concentration of ROS was subsequently detected using fluorescence microscopy. Representative images (scale bars = 200 μm) are shown. (B, C) The ROS levels of A549 cells and H1975 cells after PGD knockout or overexpression were measured assessed by flow cytometry. Representative images (left panel) and quantification (right panel) results are shown (right panel). (D) Measurement of the NADPH/$NADP^+$ ratio in A549 cells and H1975 cells after PGD knockout or overexpression. (E) Differentially enriched pathways were scored by GSVA for each cell in the PGD-low and PGD-high expression groups based on the KEGG database. (F) Knockout of PGD decreased lactate levels in A549 cells. Overexpression of PGD induced lactate production in H1975 cells. (G) The ECAR profile was monitored in PGD-overexpressing and PGD-knockout LUAD cells using a Seahorse XF96 analyzer for 100 min. (H) After PGD knockout or overexpression, A549 cells and H1975 cells were treated with oleic acid and palmitic acid (at a final concentration of 200 μM) and stained with Oil Red O.

To explore the mechanism involved in the inactivation of the AMPK pathway in LUAD patients with high PGD, we identified PGD-interacting proteins using immunoprecipitation-mass spectrometry (IP-MS) analysis in Flag-tagged PGD-overexpressing H1975 cells (Fig. 5B and C). Based on previous literature, we have summarized 26 proteins that can regulate the AMPK pathway. Among these proteins, IQGAP1 was abundantly precipitated by PGD as an interacting protein, and it was also identified as a candidate regulator of AMPK activation [32,33]. (Fig. 5D). Furthermore, Western blotting followed by coimmunoprecipitation (co-IP) confirmed that PGD interacts with IQGAP1 (Fig. 5E and F). Subsequently, the interaction between PGD and IQGAP1 was confirmed by immunofluorescence staining of H1975 cells (Fig. 5G). IQGAP1 can also bind concurrently with AMPKα to increase its phosphorylation level [34]. However, here, we found that AMPK phosphorylation was repressed after PGD overexpression, and we speculated that PGD and AMPKα may compete for IQGAP1 binding. Indeed, the interaction between IQGAP1 and AMPKα was significantly inhibited in PGD-overexpressing cells (Fig. 5H). In addition, binding domain mapping demonstrated that the IQ domain in the IQGAP1 protein, a region known to bind to AMPKα, was responsible for the interaction with PGD (Fig. 5I and J), which suggested that the IQ domain is essential for the binding of IQGAP1 and the PGD protein to block its interaction with APMKα.

3.6. Inhibition of the AMPK pathway restores the anticancer effects induced by PGD knockout

We knocked out PGD and simultaneously treated A549 cells with

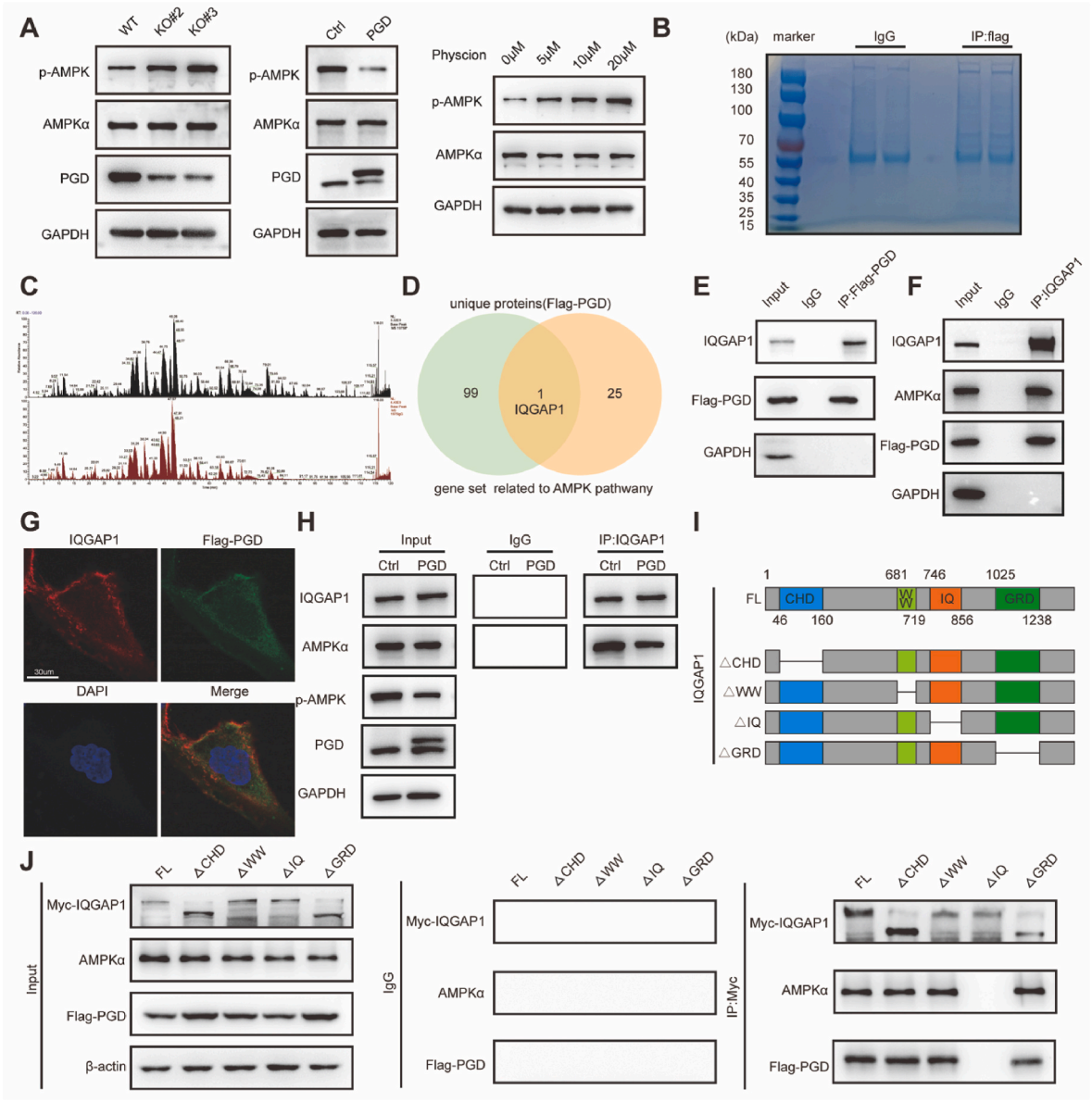

Fig. 5. PGD decreases p-AMPK levels by competitively interacting with the IQ domain of IQGAP1. (A) The levels of the indicated proteins in PGD-overexpressing, PGD-knockout or Physcion-treated LUAD cells were detected by Western blotting. (B) Proteins interacting with Flag-tagged PGD were enriched by IP, and the gel was stained with Coomassie Brilliant Blue. (C) Liquid chromatography-MS/MS was employed to identify the proteins interacting with Flag-tagged PGD. (D) Venn diagram showing the proteins identified by LC−MS/MS and an AMPK pathway-related gene set. (E) Endogenous PGD in H1975 cells was immunoprecipitated with an anti-Flag antibody, and the samples were analyzed by Western blotting using anti-Flag and anti-IQGAP1 antibodies. (F) Endogenous IQGAP1 in H1975 cells was immunoprecipitated with an anti-IQGAP1 antibody, and the samples were analyzed by Western blotting using anti-IQGAP1, anti-AMPKα and anti-Flag antibodies. (G) An immunofluorescence (IF) assay was used to detect the location of PGD and IQGAP1 in H1975 cells. (H) Endogenous IQGAP1 in Ctrl or PGD-overexpressing cells was immunoprecipitated with an anti-IQGAP1 antibody, and the samples were analyzed by Western blotting using anti-IQGAP1 and anti-AMPKα antibodies. (I) Graphic illustration of IQGAP1 deletion mutants. (J) Coimmunoprecipitation of AMPKα or PGD with full-length IQGAP1 and IQGAP1 deletion mutants tagged with Myc in HEK293 cells.

dorsomorphin dihydrochloride (an AMPK inhibitor) to confirm that PGD promoted tumor progression in an AMPK-dependent manner. Western blotting was performed to evaluate the efficiency of PGD knockout and the activity of AMPK (Fig. 6A). Knocking out PGD suppressed the proliferation of A549 cells, and this effect was reversed upon the addition of dorsomorphin dihydrochloride (Fig. 6A). Consistently, dorsomorphin dihydrochloride restored the inhibition of migration and invasion in A549 cells caused by PGD knockout (Fig. 6C). H1975 cells with PGD overexpression exhibited enhanced invasion into Matrigel, and metformin (an AMPK activator) suppressed this phenomenon (Fig. 6D). Moreover, glycolysis and fatty acid synthesis, which are regulated by the AMPK pathway, were suppressed after PGD knockout, and this inhibition effect was reversed by the addition of dorsomorphin dihydrochloride. Metformin suppressed glycolysis and fatty acid synthesis, which were upregulated by PGD (Fig. 6E–H). Thus, our data suggest that PGD may promote malignant progression via the inhibition of the AMPK pathway.

3.7. *PGD shows potential as a novel and effective therapeutic target for LUAD*

Metformin is widely used as an antidiabetic drug. In recent years, it was confirmed to inhibit tumor progression through multiple mechanisms [35–38]. In our study, it inhibited tumor proliferation in a

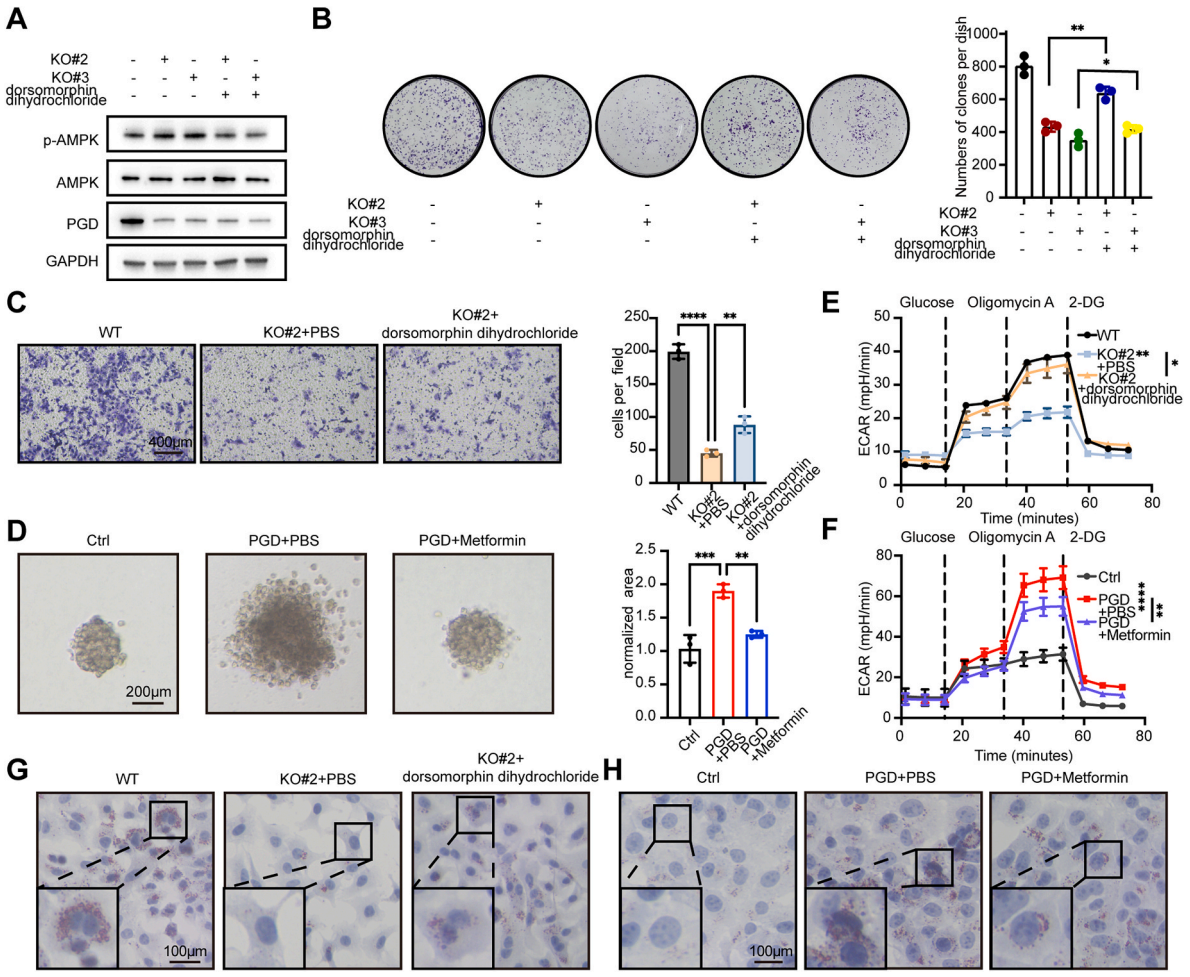

Fig. 6. PGD promotes glycolysis and fatty acid synthesis by inhibiting AMPK activation. (A) Dorsomorphin dihydrochloride rescues p-AMPK levels in PGD knockout A549 cells. (B) Representative images (left panel) and quantification results (right panel) of the colony formation abilities of PGD-knockout A549 cells treated with dorsomorphin dihydrochloride or DMSO. (C) Representative images (scale bars = 400 μm, left panel) and quantification results (right panel) of the migration abilities of PGD-knockout A549 cells treated with dorsomorphin dihydrochloride or PBS. (D) Invasion of H1975 cells after overexpression of PGD or treatment with metformin after 48 h of embedding the spheroids in Matrigel. The area occupied by spheroids embedded in Matrigel was quantified as a readout of invasion, and representative images are shown. Scale bar = 200 μm. (E, G) Inhibiting the AMPK pathway restores glycolysis and fatty acid synthesis in PGD-knockout A549 cells. (F, H) Activating the AMPK pathway rescues glycolysis and fatty acid synthesis in PGD-overexpressing H1975 cells.

dose-dependent manner (Fig. 7A). The combination of the PGD-specific inhibitor Physcion and metformin had synergistic inhibitory effects on tumor growth in vitro (Fig. 7B). We also performed tumor xenograft studies to verify the roles of the PGD and AMPK pathways in vivo. The results showed that the oral administration of both Physcion and metformin resulted in a more pronounced decrease in tumor weight and volume than did the administration of either agent alone after the subcutaneous implantation of A549 cells into nude mice (Fig. 7C–E). Furthermore, the combination exhibited the most prominent activation of the AMPK pathway (Fig. 7F). In summary, PGD and its downstream AMPK pathway are potential novel targets for the treatment of LUAD.

4. Discussion

Metabolic reprogramming is related to the occurrence and development of tumors [39–41], and the PPP is essential for maintaining the microenvironment of malignant tumors [42,43]. In the present study, through the combined analysis of single-cell data and the TCGA database, we identified significant activation of the PPP pathway in LUAD tumor cells. The rate-limiting enzymes in the PPP were found to be markedly upregulated with the malignant progression of tumors. However, only high PGD expression was associated with a poor prognosis in patients. Moreover, the impact of high PGD on prognosis was observed exclusively in LUAD patients but not in LUSC patients. The results of tissue microarray analysis confirmed this unique finding. Therefore, studying the specific effects of PGD on LUAD is particularly important given its increasing incidence in clinical settings [44].

It has been reported that PGD inhibitors are effective at inhibiting the growth and decreasing the viability of ovarian and breast cancer and leukemia cells [45,46]. In the present study, we demonstrated that PGD is vital for the proliferation, migration, and invasion abilities of LUAD cells. According to previous studies, the procarcinogenic role of PGD mainly relies on its metabolic enzyme function. NADPH is a PGD product that can combat high ROS levels [6,47,48]. High ROS levels may increase the vulnerability of cancer cells to energy and oxidative stress in the TME[49–51]. Here, we demonstrated that PGD increased the NADPH/$NADP^+$ ratio and decreased the ROS level in LUAD. Another metabolic byproduct, Ru-5-P, also promotes carcinogenesis. The inhibition of PGD activity reduced the Ru-5-P content to levels below physiological concentrations and activated the LKB1/AMPK pathway, leading to decreased ACC1 enzyme activity [8,46]. ACC1 plays an important role in lipid synthesis, a critical metabolic process in rapidly growing tumors [52]. Moreover, the AMPK pathway inhibits tumor growth by suppressing glycolysis via the inhibition of HIF1α-HK2

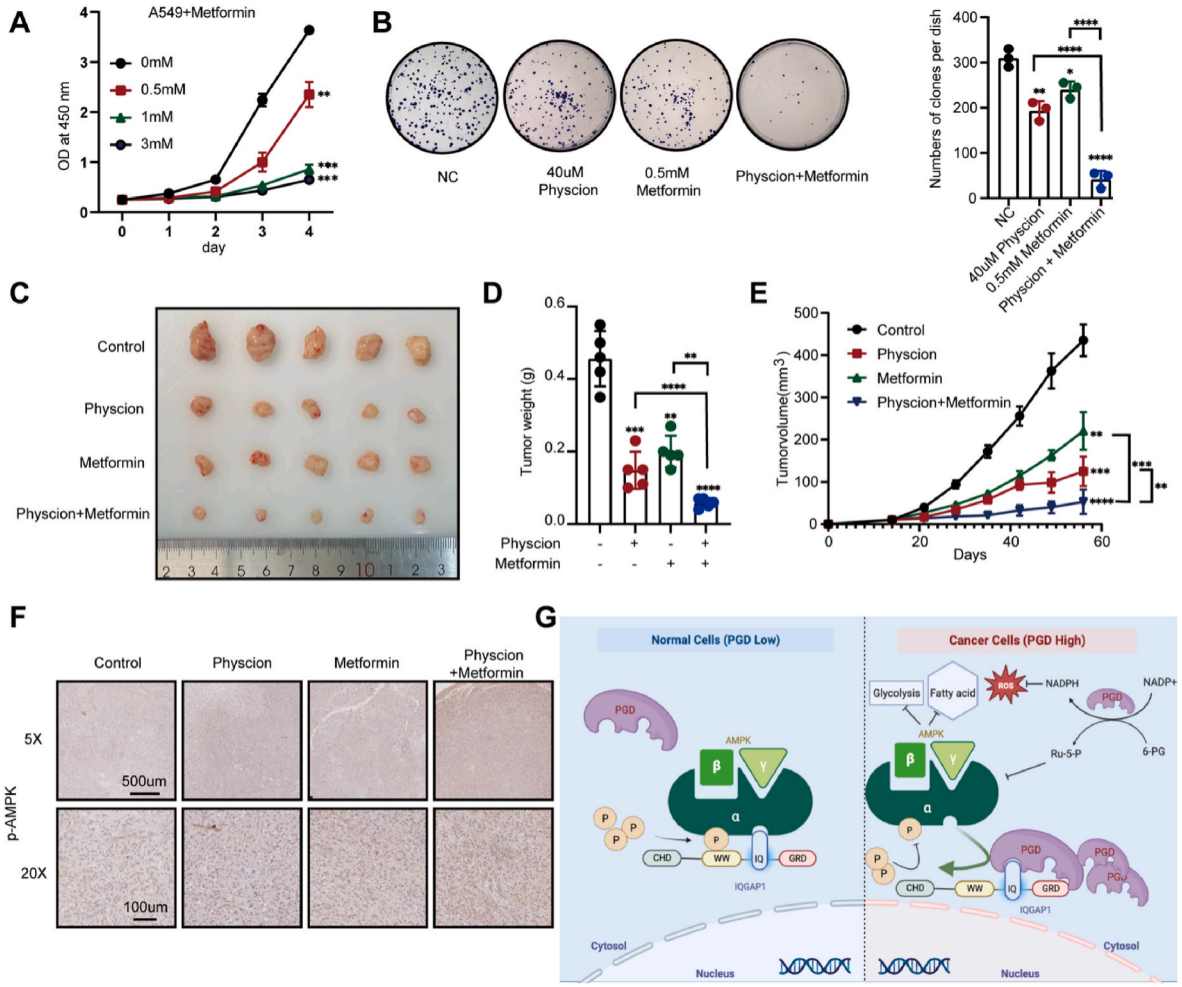

Fig. 7. The clinical significance of the PGD/AMPK axis in LUAD. (A) Metformin decreased cell viability in a concentration-dependent manner. (B) Representative images (left panel) and quantification results (right panel) of the colony formation abilities of A549 cells treated with Physcion, metformin, or both. (C) Oral administration of Physcion, metformin, or both inhibited the growth of subcutaneous tumors derived from A549 LUAD cells in nude mice (n = 5). (D) After the mice were euthanized, the tumors were extracted and weighed. (E) The tumor volume was monitored every other day, and tumor growth curves were generated. (F) Tumor sections were stained with anti-p-AMPK antibodies and assessed by IHC (scale bars = 100/500 μm). (G) Graphical illustration of the PGD-mediated modulation of tumor glycolysis and fatty acid synthesis, which promotes tumor growth.

expression [53]. HK2, a pivotal enzyme, facilitates aerobic glycolysis and orchestrates the reconfiguration of metabolic pathways in cancer cells [54–56]. According to the findings from the single-cell analysis, we divided epithelial cells into two groups based on the expression levels of PGD and performed enrichment analysis using the KEGG dataset. The results showed significant enrichment in the adipocytokine signaling pathway and the glycolysis pathway.

In clinical settings, LUAD patients often exhibit mutations in LKB1 and are prone to metastasis and metabolic disorders [57]. Therefore, we hypothesized that PGD may promote cancer progression independent of its enzymatic function. To explore this further, we utilized IP-MS to identify proteins that interact with PGD. Here, we first identified a specific interaction between PGD and IQGAP1 that could activate the AMPK pathway by regulating CaMKK2 [34]. Then, by overexpressing IQGAP1 fragments lacking different domains, we demonstrated that the binding site on IQGAP1 was located within the IQ domain, which is the region known to bind to AMPKα.

These results demonstrated the critical role of PGD in the AMPK pathway in LUAD progression. However, there are still some limitations to our study. The limited number of single-cell sequencing samples may introduce slight biases to the conclusion. Moreover, PGD could modulate the malignant progression of tumors through mechanisms independent of the PPP or binding proteins, such as the activation of the receptor tyrosine kinase c-Met [58], which needs to be explored further.

In conclusion, our study demonstrated that PGD is upregulated in LUAD and inhibits the AMPK pathway, whereby it enhances glycolysis and fatty acid synthesis to promote the malignant progression of tumors. Thus, targeting PGD is a potential therapeutic strategy for the treatment of LUAD.

Consent for publication

Not applicable.

Funding

This study was supported by the Jiangsu Provincial Health Commission Research Project on Elderly Health (LKZ2022019), Yangzhou Social Development and Clinical Frontier Technology Project (YZ2023084), Yangzhou Innovation Capability Building Design Plan Project (YZ2022168) and Yangzhou Social Development and Clinical Frontier Technology Project (YZ2021078).

Data statement

The raw sequence data reported in this paper have been deposited in

the Genome Sequence Archive (Genomics, Proteomics & Bioinformatics 2021) in National Genomics Data Center (Nucleic Acids Res 2021), China National Center for Bioinformation/Beijing Institute of Genomics, Chinese Academy of Sciences (GSA: HRA006859) that are publicly accessible at https://ngdc.cncb.ac.cn/gsa. The data are available upon reasonable request.

CRediT authorship contribution statement

Jun Wu: Writing – original draft, Data curation, Conceptualization. **Yong Chen:** Validation, Software. **Hui Zou:** Formal analysis. **Kaiyue Xu:** Visualization, Conceptualization. **Jiaqi Hou:** Data curation. **Mengmeng Wang:** Data curation. **Shuyu Tian:** Data curation. **Mingjun Gao:** Data curation. **Qinglin Ren:** Data curation. **Chao Sun:** Data curation. **Shichun Lu:** Data curation. **Qiang Wang:** Conceptualization. **Yusheng Shu:** Methodology, Formal analysis. **Shouyu Wang:** Conceptualization. **Xiaolin Wang:** Writing – review & editing, Conceptualization.

Declaration of competing interest

The authors declare that they have no known competing financial interests or personal relationships that could have appeared to influence the work reported in this paper.

Appendix A. Supplementary data

Supplementary data to this article can be found online at https://doi.org/10.1016/j.canlet.2024.217177.

References

[1] R.L. Siegel, A.N. Giaquinto, A. Jemal, Cancer statistics, CA A Cancer J. Clin. 74 (2024) 12–49, https://doi.org/10.3322/caac.21820, 2024.

[2] R.L. Siegel, K.D. Miller, N.S. Wagle, A. Jemal, Cancer statistics, CA A Cancer J. Clin. 73 (2023) 17–48, https://doi.org/10.3322/caac.21763, 2023.

[3] J. Li, L. Zhu, H.F. Kwok, Nanotechnology-based approaches overcome lung cancer drug resistance through diagnosis and treatment, Drug Resist. Updat. Rev. Comment. Antimicrob. Anticancer Chemother. 66 (2023) 100904, https://doi.org/10.1016/j.drup.2022.100904.

[4] J. Ren, B. Ren, X. Liu, M. Cui, Y. Fang, X. Wang, F. Zhou, M. Gu, R. Xiao, J. Bai, L. You, Y. Zhao, Crosstalk between metabolic remodeling and epigenetic reprogramming: a new perspective on pancreatic cancer, Cancer Lett. 587 (2024) 216649, https://doi.org/10.1016/j.canlet.2024.216649.

[5] Targeting cancer metabolic pathways for improving chemotherapy and immunotherapy - PubMed, (n.d.). https://pubmed.ncbi.nlm.nih.gov/37739209/ (accessed April 24, 2024).

[6] K.C. Patra, N. Hay, The pentose phosphate pathway and cancer, Trends Biochem. Sci. 39 (2014) 347–354, https://doi.org/10.1016/j.tibs.2014.06.005.

[7] R. Lin, S. Elf, C. Shan, H.-B. Kang, Q. Ji, L. Zhou, T. Hitosugi, L. Zhang, S. Zhang, J. Ho Seo, J. Xie, M. Tucker, T.-L. Gu, J. Sudderth, L. Jiang, M. Mitsche, R. J. DeBerardinis, S. Wu, Y. Li, H. Mao, P.R. Chen, D. Wang, G.Z. Chen, S.J. Hurwitz, S. Lonial, H.J. Khoury, M.L. Arellano, H.J. Khoury, F.R. Khuri, B.H. Lee, Q. Lei, D. J. Brat, K. Ye, T.J. Boggon, C. He, S. Kang, J. Fan, J. Chen, 6-phosphogluconate dehydrogenase links oxidative PPP, lipogenesis and tumor growth by inhibiting LKB1-AMPK signaling, Nat. Cell Biol. 17 (2015) 1484–1496, https://doi.org/10.1038/ncb3255.

[8] C. Shan, S. Elf, Q. Ji, H.-B. Kang, L. Zhou, T. Hitosugi, L. Jin, R. Lin, L. Zhang, J. H. Seo, J. Xie, M. Tucker, T.-L. Gu, J. Sudderth, L. Jiang, R.J. DeBerardinis, S. Wu, Y. Li, H. Mao, P.R. Chen, D. Wang, G.Z. Chen, S. Lonial, M.L. Arellano, H.J. Khoury, F.R. Khuri, B.H. Lee, D.J. Brat, K. Ye, T.J. Boggon, C. He, S. Kang, J. Fan, J. Chen, Lysine acetylation activates 6-phosphogluconate dehydrogenase to promote tumor growth, Mol. Cell 55 (2014) 552–565, https://doi.org/10.1016/j.molcel.2014.06.020.

[9] R. Liu, W. Li, B. Tao, X. Wang, Z. Yang, Y. Zhang, C. Wang, R. Liu, H. Gao, J. Liang, W. Yang, Tyrosine phosphorylation activates 6-phosphogluconate dehydrogenase and promotes tumor growth and radiation resistance, Nat. Commun. 10 (2019) 991, https://doi.org/10.1038/s41467-019-08921-8.

[10] F. Zhang, Z. Wu, B. Yu, Z. Ning, Z. Lu, L. Li, F. Long, Q. Hu, C. Zhong, Y. Zhang, C. Lin, ATP13A2 activates the pentose phosphate pathway to promote colorectal cancer growth though TFEB-PGD axis, Clin. Transl. Med. 13 (2023) e1272, https://doi.org/10.1002/ctm2.1272.

[11] J.L. Gillis, J.A. Hinneh, N.K. Ryan, S. Irani, M. Moldovan, L.-E. Quek, R.K. Shrestha, A.R. Hanson, J. Xie, A.J. Hoy, J. Holst, M.M. Centenera, I.G. Mills, D.J. Lynn, L. A. Selth, L.M. Butler, A feedback loop between the androgen receptor and 6-phosphogluconate dehydrogenase (6PGD) drives prostate cancer growth, Elife 10 (2021) e62592, https://doi.org/10.7554/eLife.62592.

[12] J.M. Smith, A.C. Hedman, D.B. Sacks, IQGAPs choreograph cellular signaling from the membrane to the nucleus, Trends Cell Biol. 25 (2015) 171–184, https://doi.org/10.1016/j.tcb.2014.12.005.

[13] H.-F. Hu, G.-B. Gao, X. He, Y.-Y. Li, Y.-J. Li, B. Li, Y. Pan, Y. Wang, Q.-Y. He, Targeting ARF1-IQGAP1 interaction to suppress colorectal cancer metastasis and vemurafenib resistance, J. Adv. Res. 51 (2023) 135–147, https://doi.org/10.1016/j.jare.2022.11.006.

[14] A.C. Hedman, Z. Li, L. Gorisse, S. Parvathaneni, C.J. Morgan, D.B. Sacks, IQGAP1 binds AMPK and is required for maximum AMPK activation, J. Biol. Chem. 296 (2020) 100075, https://doi.org/10.1074/jbc.RA120.016193.

[15] M. Capula, M. Perán, G. Xu, V. Donati, D. Yee, A. Gregori, Y.G. Assaraf, E. Giovannetti, D. Deng, Role of drug catabolism, modulation of oncogenic signaling and tumor microenvironment in microbe-mediated pancreatic cancer chemoresistance, Drug Resist. Updat. Rev. Comment. Antimicrob. Anticancer Chemother. 64 (2022) 100864, https://doi.org/10.1016/j.drup.2022.100864.

[16] S. Zhou, J. Zheng, W. Zhai, Y. Chen, Spatio-temporal heterogeneity in cancer evolution and tumor microenvironment of renal cell carcinoma with tumor thrombus, Cancer Lett. 572 (2023) 216350, https://doi.org/10.1016/j.canlet.2023.216350.

[17] J.E. Bader, K. Voss, J.C. Rathmell, Targeting metabolism to improve the tumor microenvironment for cancer immunotherapy, Mol. Cell 78 (2020) 1019–1033, https://doi.org/10.1016/j.molcel.2020.05.034.

[18] Z. Liu, D. Wang, J. Zhang, P. Xiang, Z. Zeng, W. Xiong, L. Shi, cGAS-STING signaling in the tumor microenvironment, Cancer Lett. 577 (2023) 216409, https://doi.org/10.1016/j.canlet.2023.216409.

[19] N.N. Pavlova, C.B. Thompson, The emerging hallmarks of cancer metabolism, Cell Metabol. 23 (2016) 27–47, https://doi.org/10.1016/j.cmet.2015.12.006.

[20] A. Liberzon, C. Birger, H. Thorvaldsdóttir, M. Ghandi, J.P. Mesirov, P. Tamayo, The Molecular Signatures Database (MSigDB) hallmark gene set collection, Cell Syst. 1 (2015) 417–425, https://doi.org/10.1016/j.cels.2015.12.004.

[21] S. K, R. D, F. Rb, D. D, N. J, Y. N, P. E, D. S, Slingshot: cell lineage and pseudotime inference for single-cell transcriptomics, BMC Genom. 19 (2018), https://doi.org/10.1186/s12864-018-4772-0.

[22] N. Hay, Reprogramming glucose metabolism in cancer: can it be exploited for cancer therapy? Nat. Rev. Cancer 16 (2016) 635–649, https://doi.org/10.1038/nrc.2016.77.

[23] V. Sosa, T. Moliné, R. Somoza, R. Paciucci, H. Kondoh, M.E. Lleonart, Oxidative stress and cancer: an overview, Ageing Res. Rev. 12 (2013) 376–390, https://doi.org/10.1016/j.arr.2012.10.004.

[24] S. Prasad, S.C. Gupta, A.K. Tyagi, Reactive oxygen species (ROS) and cancer: role of antioxidative nutraceuticals, Cancer Lett. 387 (2017) 95–105, https://doi.org/10.1016/j.canlet.2016.03.042.

[25] M. Dodson, V. Darley-Usmar, J. Zhang, Cellular metabolic and autophagic pathways: traffic control by redox signaling, Free Radic. Biol. Med. 63 (2013) 207–221, https://doi.org/10.1016/j.freeradbiomed.2013.05.014.

[26] M.S. Hernandes, L.R.G. Britto, NADPH oxidase and neurodegeneration, Curr. Neuropharmacol. 10 (2012) 321–327, https://doi.org/10.2174/157015912804143540.

[27] D. Garcia, R.J. Shaw, AMPK: mechanisms of cellular energy sensing and restoration of metabolic balance, Mol. Cell 66 (2017) 789–800, https://doi.org/10.1016/j.molcel.2017.05.032.

[28] J. Ha, K.-L. Guan, J. Kim, AMPK and autophagy in glucose/glycogen metabolism, Mol. Aspect. Med. 46 (2015) 46–62, https://doi.org/10.1016/j.mam.2015.08.002.

[29] S.-C. Lin, D.G. Hardie, AMPK: sensing glucose as well as cellular energy status, Cell Metabol. 27 (2018) 299–313, https://doi.org/10.1016/j.cmet.2017.10.009.

[30] H. Chen, D. Wu, L. Bao, T. Yin, D. Lei, J. Yu, X. Tong, 6PGD inhibition sensitizes hepatocellular carcinoma to chemotherapy via AMPK activation and metabolic reprogramming, Biomed. Pharmacother. Biomedecine Pharmacother. 111 (2019) 1353–1358, https://doi.org/10.1016/j.biopha.2019.01.028.

[31] J. Cao, X. Sun, X. Zhang, D. Chen, 6PGD upregulation is associated with chemo- and immuno-resistance of renal cell carcinoma via AMPK signaling-dependent NADPH-mediated metabolic reprograming, Am. J. Med. Sci. 360 (2020) 279–286, https://doi.org/10.1016/j.amjms.2020.06.014.

[32] E.F. Trefts, R.J. Shaw, AMPK: restoring metabolic homeostasis over space and time, Mol. Cell 81 (2021) 3677–3690, https://doi.org/10.1016/j.molcel.2021.08.015.

[33] S. Herzig, R.J. Shaw, AMPK: guardian of metabolism and mitochondrial homeostasis, Nat. Rev. Mol. Cell Biol. 19 (2018) 121–135, https://doi.org/10.1038/nrm.2017.95.

[34] A.C. Hedman, Z. Li, L. Gorisse, S. Parvathaneni, C.J. Morgan, D.B. Sacks, IQGAP1 binds AMPK and is required for maximum AMPK activation, J. Biol. Chem. 296 (2020) 100075, https://doi.org/10.1074/jbc.RA120.016193.

[35] G. Wang, H. Gao, S. Dai, M. Li, Y. Gao, L. Yin, K. Zhang, J. Zhang, K. Jiang, Y. Miao, Z. Lu, Metformin inhibits neutrophil extracellular traps-promoted pancreatic carcinogenesis in obese mice, Cancer Lett. 562 (2023) 216155, https://doi.org/10.1016/j.canlet.2023.216155.

[36] X. Huang, T. Sun, J. Wang, X. Hong, H. Chen, T. Yan, C. Zhou, D. Sun, C. Yang, T. Yu, W. Su, W. Du, H. Xiong, Metformin reprograms tryptophan metabolism to stimulate CD8+ T-cell function in colorectal cancer, Cancer Res. 83 (2023) 2358–2371, https://doi.org/10.1158/0008-5472.CAN-22-3042.

[37] T.E. LaMoia, G.I. Shulman, Cellular and molecular mechanisms of metformin action, Endocr. Rev. 42 (2021) 77–96, https://doi.org/10.1210/endrev/bnaa023.

[38] I. Pernicova, M. Korbonits, Metformin–mode of action and clinical implications for diabetes and cancer, Nat. Rev. Endocrinol. 10 (2014) 143–156, https://doi.org/10.1038/nrendo.2013.256.

[39] M.G. Vander Heiden, R.J. DeBerardinis, Understanding the intersections between metabolism and cancer biology, Cell 168 (2017) 657–669, https://doi.org/10.1016/j.cell.2016.12.039.
[40] Z. Li, C. Sun, Z. Qin, Metabolic reprogramming of cancer-associated fibroblasts and its effect on cancer cell reprogramming, Theranostics 11 (2021) 8322–8336, https://doi.org/10.7150/thno.62378.
[41] L. Xia, L. Oyang, J. Lin, S. Tan, Y. Han, N. Wu, P. Yi, L. Tang, Q. Pan, S. Rao, J. Liang, Y. Tang, M. Su, X. Luo, Y. Yang, Y. Shi, H. Wang, Y. Zhou, Q. Liao, The cancer metabolic reprogramming and immune response, Mol. Cancer 20 (2021) 28, https://doi.org/10.1186/s12943-021-01316-8.
[42] J. Cheng, Y. Huang, X. Zhang, Y. Yu, S. Wu, J. Jiao, L. Tran, W. Zhang, R. Liu, L. Zhang, M. Wang, M. Wang, W. Yan, Y. Wu, F. Chi, P. Jiang, X. Zhang, H. Wu, TRIM21 and PHLDA3 negatively regulate the crosstalk between the PI3K/AKT pathway and PPP metabolism, Nat. Commun. 11 (2020) 1880, https://doi.org/10.1038/s41467-020-15819-3.
[43] P. Jiang, W. Du, M. Wu, Regulation of the pentose phosphate pathway in cancer, Protein Cell 5 (2014) 592–602, https://doi.org/10.1007/s13238-014-0082-8.
[44] P. Chen, Y. Liu, Y. Wen, C. Zhou, Non-small cell lung cancer in China, Cancer Commun, Lond. Engl. 42 (2022) 937–970, https://doi.org/10.1002/cac2.12359.
[45] W. Zheng, Q. Feng, J. Liu, Y. Guo, L. Gao, R. Li, M. Xu, G. Yan, Z. Yin, S. Zhang, S. Liu, C. Shan, Inhibition of 6-phosphogluconate dehydrogenase reverses cisplatin resistance in ovarian and lung cancer, Front. Pharmacol. 8 (2017) 421, https://doi.org/10.3389/fphar.2017.00421.
[46] X. Yang, X. Peng, J. Huang, Inhibiting 6-phosphogluconate dehydrogenase selectively targets breast cancer through AMPK activation, Clin. Transl. Oncol. Off. Publ. Fed. Span. Oncol. Soc. Natl. Cancer Inst. Mex. 20 (2018) 1145–1152, https://doi.org/10.1007/s12094-018-1833-4.
[47] H.-Q. Ju, J.-F. Lin, T. Tian, D. Xie, R.-H. Xu, NADPH homeostasis in cancer: functions, mechanisms and therapeutic implications, Signal Transduct. Targeted Ther. 5 (2020) 231, https://doi.org/10.1038/s41392-020-00326-0.
[48] L. Chen, Z. Zhang, A. Hoshino, H.D. Zheng, M. Morley, Z. Arany, J.D. Rabinowitz, NADPH production by the oxidative pentose-phosphate pathway supports folate metabolism, Nat. Metab. 1 (2019) 404–415.
[49] S.J. Forrester, D.S. Kikuchi, M.S. Hernandes, Q. Xu, K.K. Griendling, Reactive oxygen species in metabolic and inflammatory signaling, Circ. Res. 122 (2018) 877–902, https://doi.org/10.1161/CIRCRESAHA.117.311401.
[50] P. Chen, X. Zhong, Y. Song, W. Zhong, S. Wang, J. Wang, P. Huang, Y. Niu, W. Yang, Z. Ding, Q. Luo, C. Yang, J. Wang, W. Zhang, Triptolide induces apoptosis and cytoprotective autophagy by ROS accumulation via directly targeting peroxiredoxin 2 in gastric cancer cells, Cancer Lett. 587 (2024) 216622, https://doi.org/10.1016/j.canlet.2024.216622.
[51] E.C. Cheung, K.H. Vousden, The role of ROS in tumour development and progression, Nat. Rev. Cancer 22 (2022) 280–297, https://doi.org/10.1038/s41568-021-00435-0.
[52] S.M. Hadad, D.G. Hardie, V. Appleyard, A.M. Thompson, Effects of metformin on breast cancer cell proliferation, the AMPK pathway and the cell cycle, Clin. Transl. Oncol. Off. Publ. Fed. Span. Oncol. Soc. Natl. Cancer Inst. Mex. 16 (2014) 746–752, https://doi.org/10.1007/s12094-013-1144-8.
[53] C. Xu, Q. Hong, K. Zhuang, X. Ren, S. Cui, Z. Dong, Q. Wang, X. Bai, X. Chen, Regulation of pericyte metabolic reprogramming restricts the AKI to CKD transition, Metabolism 145 (2023) 155592, https://doi.org/10.1016/j.metabol.2023.155592.
[54] V.P. Tan, S. Miyamoto, HK2/hexokinase-II integrates glycolysis and autophagy to confer cellular protection, Autophagy 11 (2015) 963–964, https://doi.org/10.1080/15548627.2015.1042195.
[55] F. Hinrichsen, J. Hamm, M. Westermann, L. Schröder, K. Shima, N. Mishra, A. Walker, N. Sommer, K. Klischies, D. Prasse, J. Zimmermann, S. Kaiser, D. Bordoni, A. Fazio, G. Marinos, G. Laue, S. Imm, V. Tremaroli, M. Basic, R. Häsler, R.A. Schmitz, S. Krautwald, A. Wolf, B. Stecher, P. Schmitt-Kopplin, C. Kaleta, J. Rupp, F. Bäckhed, P. Rosenstiel, F. Sommer, Microbial regulation of hexokinase 2 links mitochondrial metabolism and cell death in colitis, Cell Metabol. 33 (2021) 2355–2366.e8, https://doi.org/10.1016/j.cmet.2021.11.004.
[56] M.F. Bustamante, P.G. Oliveira, R. Garcia-Carbonell, A.P. Croft, J.M. Smith, R. L. Serrano, E. Sanchez-Lopez, X. Liu, T. Kisseleva, N. Hay, C.D. Buckley, G. S. Firestein, A.N. Murphy, S. Miyamoto, M. Guma, Hexokinase 2 as a novel selective metabolic target for rheumatoid arthritis, Ann. Rheum. Dis. 77 (2018) 1636–1643, https://doi.org/10.1136/annrheumdis-2018-213103.
[57] J. Kim, H.M. Lee, F. Cai, B. Ko, C. Yang, E.L. Lieu, N. Muhammad, S. Rhyne, K. Li, M. Haloul, W. Gu, B. Faubert, A.K. Kaushik, L. Cai, S. Kasiri, U. Marriam, K. Nham, L. Girard, H. Wang, X. Sun, J. Kim, J.D. Minna, K. Unsal-Kacmaz, R.J. DeBerardinis, The hexosamine biosynthesis pathway is a targetable liability in KRAS/LKB1 mutant lung cancer, Nat. Metab. 2 (2020) 1401–1412, https://doi.org/10.1038/s42255-020-00316-0.
[58] B. Chan, P.A. VanderLaan, V.P. Sukhatme, 6-Phosphogluconate dehydrogenase regulates tumor cell migration in vitro by regulating receptor tyrosine kinase c-Met, Biochem. Biophys. Res. Commun. 439 (2013) 247–251, https://doi.org/10.1016/j.bbrc.2013.08.048.